KKU Engineering Journal

https://www.tci-thaijo.org/index.php/kkuenj/index

Effect of various dimensions of cyclone combustor to burn raw producer gas

Chintara Raepet and Kiatfa Tangchaichit*

Research Unit on Mechanical Component Design, Department of Mechanical Engineering, Faculty of Engineering, Khon Kaen University, Khon Kaen 40002, Thailand.

Received April 2016
Accepted June 2016

Abstract

A cyclone combustor was designed for syngas combustion induce in this paper. The syngas from biomass gasification is burned in cyclone combustor as a fuel. The objective of this research is to investigate the effects of various dimension of cyclone chamber including different diameters and different lengths of cyclone combustion chamber. The tangential velocity and exhaust gas quality are compared in various dimension of cyclone chamber. The result shows that the small diameter and long chamber of combustor cause high burning efficiency; the combustor can produce high CO2, low O2 and high exhaust gas temperature. To produce strongly cyclonic flow, the combustor should have large diameter and short length.

Keywords: Cyclone combustor, Raw producer gas, Numerical simulation

1. Introduction

Gasification technology is an important combustion process converting biomass based on carbonaceous compound into hydrogen, carbon monoxide and carbon dioxide [1-3]. Low heating value gas derived from biomass gasification requires a high resident time in combustion process. Cyclone combustor is presented as a combustor to burn biomass gaseous fuel with respect to increase resident time [4-5]. The advantages of cyclone concept enhance flame stability because rapidly mixing of air and fuel, resident time and suitable with low calorific value fuel gas [6-7]. In addition, cyclone combustor is applied to burn gas from gasification process to reduce a cooling and cleaning procedure (such as gas cooler, scrubber, chiller, fabric filter, water treatment and so on).

The main objective of this research is to investigate the effects of the dimension of combustion chamber (by changing diameter and length of combustion chamber) by using Computation Fluid Dynamics (CFD) simulation.

2. Numerical modelling

2.1 Condition and considered cyclone combustor dimensions

The reference case is compared with experimental data obtained by S. Dattarajan et al. [8]. The dimensions are 391 mm chamber diameter (D), 591 mm chamber length (L), air and fuel inlet 60 x 100 mm square pipes. Fuel and air inlet are set in Table 1 and typical raw producer gas from gasifier as a fuel (12 % H_2, 21% CO, 1.5% CH_4, 10% CO_2, 4% H_2O and 47.5% N_2 by volume). Number of elements for this case are 0.13, 0.4, 0.7 and 1 million cells and 0.7 million cells are chosen for the optimum size.

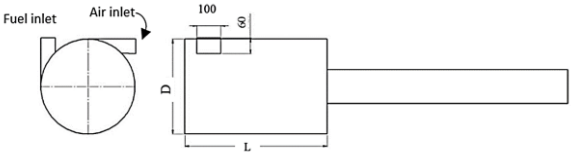

Figure 1 Schematic diagram of the cyclone combustor. Dimensions shown are in mm.

Table 1 Inlet conditions

Fuel (kg/hr)	*Air (kg/hr)*	*Temp fuel (°C)*	*Temp air (°C)*	*Equivalent ratio (λ)*
52.2	75.4	302	304	1.21

The combustor is designed to create the cyclonic flow. In this research, aim to investigate the effect of geometries with various chamber diameters (D) and lengths (L). The following twelve design geometries (Table 2) are investigated. Diameters and lengths are decreased and increased from reference case (M6 in Table 2).

2.2 Simulation approaches

Numerical simulation of cyclone gaseous combustion has been performed using ANSYS Fluent 14.5. In this research, Reynolds Stress Model (RSM) has been used for

*Corresponding author. Tel.: +6683 415 7715
Email address: kiatfa@kkumail.com
doi: 10.14456/kkuenj.2016.140

Table 2 Designed chamber dimensions (D and L are dimensions of combustor, see in Figure 1)

Model	*M1*	*M2*	*M3*	*M4*	*M5*	*M6*	*M7*	*M8*	*M9*	*M10*	*M11*	*M12*
D (mm)	250	250	250	250	391	391	391	391	600	600	600	600
L (mm)	300	591	900	1200	300	591	900	1200	300	591	900	1200

turbulence modelling to solve flow field for RANS (Reynolds-averaged Navier-Strokes equations) simulation. The steady state governing equations for continuity and momentum can be written in Cartesian coordinates as [9-10]:

$$\frac{\partial}{\partial x_i}(\rho u_i) = 0 \tag{1}$$

$$\frac{\partial}{\partial x_i}(\rho u_i u_j) = -\frac{\partial p}{\partial x_i} + \frac{\partial}{\partial x_j}\left[\mu\left(\frac{\partial u_i}{\partial x_j} + \frac{\partial u_j}{\partial x_i} - \frac{2}{3}\delta_{ij}\frac{\partial u_i}{\partial x_i}\right)\right] + \frac{\partial}{\partial x_j}\left(-\rho\overline{u_i' u_j'}\right) \tag{2}$$

Where ρ is the density, $u_{i/j}$ is the velocity vector components, p is pressure. Reynolds stresses are related to the average velocity gradients using the Boussinesq hypothesis:

$$-\rho\overline{u_i' u_j'} = \mu_t\left(\frac{\partial u_i}{\partial x_j} + \frac{\partial u_j}{\partial x_i}\right) - \frac{2}{3}\left(\rho k + \mu_t\frac{\partial u_i}{\partial x_i}\right)\delta_{ij} \tag{3}$$

μ_t represents the turbulent dynamic viscosity and k is the turbulence kinetic energy.

The turbulence chemistry interaction has been modeled using non-premixed combustion model based on the probability density function (PDF) [11-12]. The instantaneous thermochemical state of the fluid for non-premixed modeling is related to a conserved scalar quantity that is the mixture fraction f. The mixture fraction can be written in terms of the atomic mass fraction as

$$f = \frac{Y_i - Y_{i,ox}}{Y_{i,\,fuel} - Y_{i,ox}} \tag{4}$$

Where Y_i is the mass fraction for element *i*. The subscript OX is the value at the oxidizer stream inlet and the subscript fuel is the value at the fuel stream inlet. In the PDF model, species equations solved for each species is reduced to a single equation for mixture fraction f that under the assumption of equal diffusivities. The Favre mean (density-averaged) mixture fraction equation is

$$\nabla\cdot\left(\rho\vec{v}\overline{f}\right) = \nabla\cdot\left(\frac{\mu_t}{\sigma_t}\nabla\overline{f}\right) \tag{5}$$

To solving a conservation equation the mixture fraction variance $\overline{f'^2}$ is also required.

$$\nabla\cdot\left(\rho\vec{v}\,\overline{f'^2}\right) = \nabla\cdot\left(\frac{\mu_t}{\sigma_t}\nabla\overline{f'^2}\right) + C_g\mu_t\cdot\left(\nabla\overline{f}\right)^2 - C_d\rho\frac{\varepsilon}{k}\overline{f'^2} \tag{6}$$

Where $f' = f - \bar{f}$. The constant values σ_t, C_g and C_d are 0.85, 2.86 and 2.0 respectively. The energy equation is solved for non-adiabatic non-premixed combustion model as [13]:

$$\nabla\cdot\left(\rho\vec{v}H\right) = \nabla\cdot\left(\frac{k_t}{c_p}\nabla H\right) + S_h \tag{7}$$

Where k_t is the turbulent thermal conductivity and S_h is heat of chemical reaction. The modeling of turbulence-chemistry interaction using PDF donates as $p(f)$ computed for density-weighted mean species mass fractions and temperature:

$$\bar{\phi}_i = \int_0^1 p(f)\phi(f,H)df \tag{8}$$

Where $\emptyset(f,H)$ is the instantaneous value of the thermo-chemical scalars (species, density and temperature). According to description above, these computational procedure can be found in standard texts on turbulence combustion [14] and Ansys fluent theory guide [15].

Boundary conditions at the fuel and air inlets for all models are set to fixed values list in Table 1. The combustor walls are treated as adiabatic. The mesh size is set at the same size of reference case. A computer with Xeon CPU and 56 GB of RAM is used to perform these computations.

3. Results and discussion

3.1 Reference case

As displays in Figure 2 shows current numerical simulation of cyclone combustor are compared with experimental and numerical results obtained by S. Dattarajan et al. that agreement between experimental and numerical data of temperature is less along the combustor centerline and improves as one moves closer the wall. The current CFD and experimental data obtained by S. Dattarajan et al. fairly close for temperature in combustor. As shows in Figure 3 is observed that the temperature at center axis is rather difference because the high tangential velocity cause difficult to measure.

3.2 Tangential velocity

In Figure 3, shows the tangential velocity profile at three different axial locations in the combustors. The tangential velocity increases from minimum at the center of combustor and reaches to maximum at the 1/4 radius away from the center of combustor. The vortex structure due to tangential velocity reaches fully developed configuration by large diameter and small length of combustor that can be seen in model M5 and M9. Other models are not reached to fully vortex structure because the inlet pipes are asymmetry.

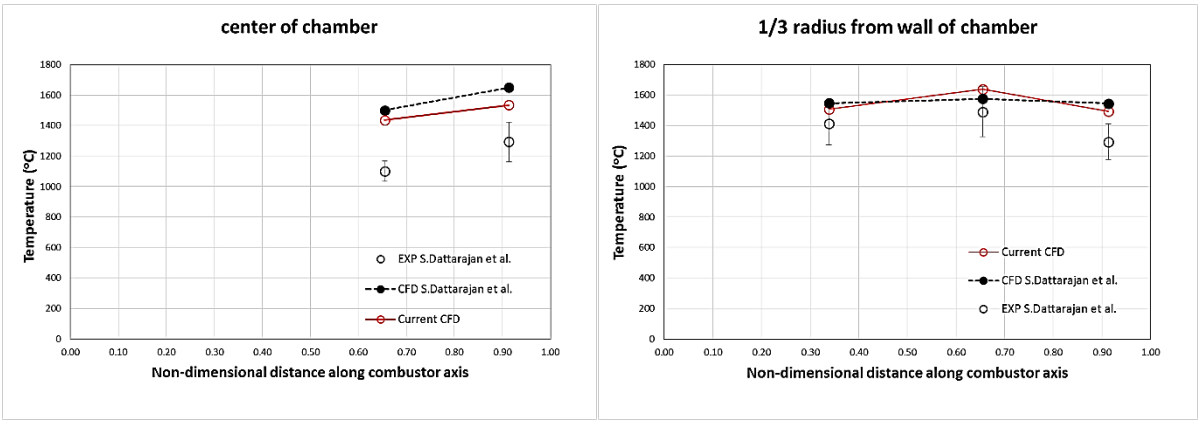

(a) (b)

Figure 2 Comparison of CFD with experiment, the temperature at (a) center axis and (b) 1/3 radius from wall of chamber.

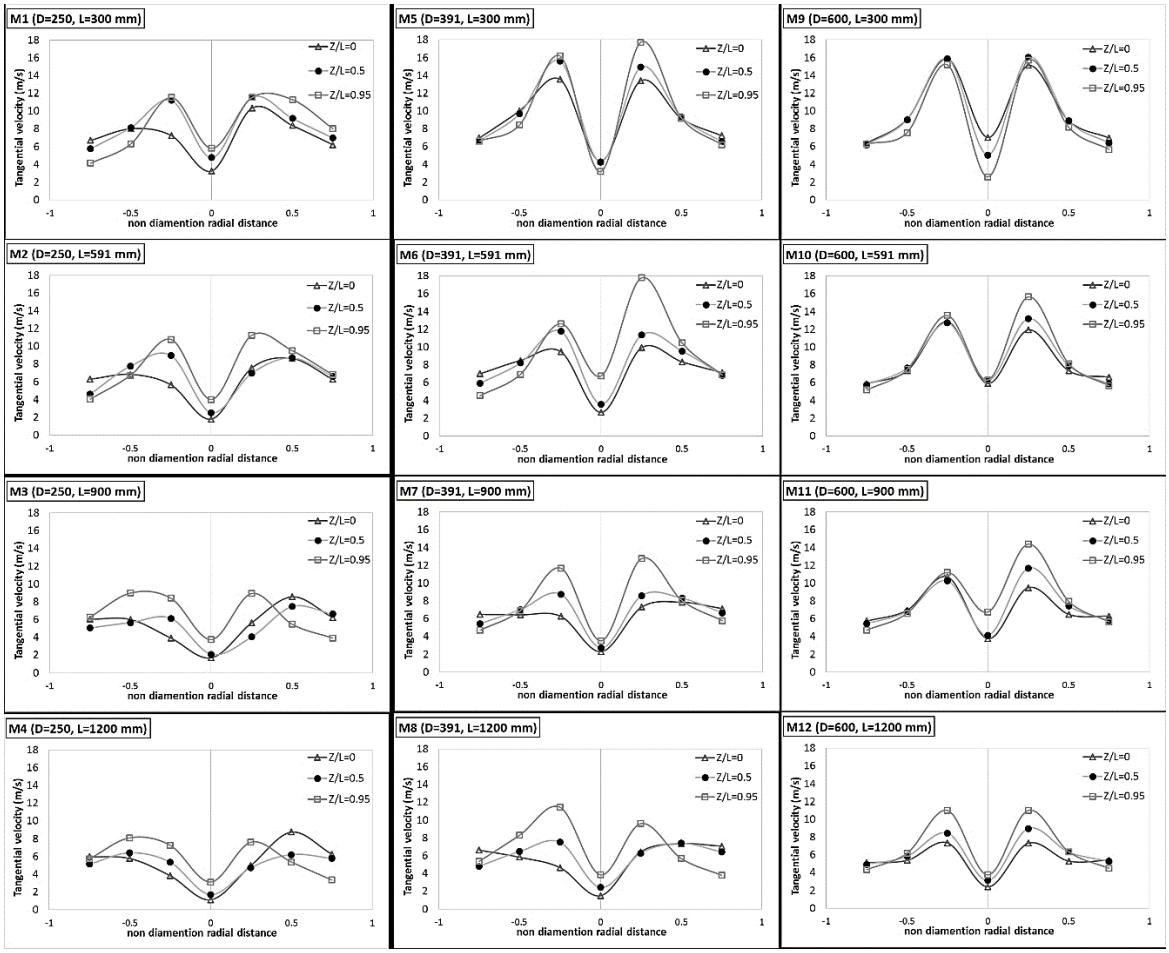

Figure 3 Predicted tangential velocity profiles at different axial distances with difference dimensions (Z is distance from mid-plane of inlet pipe and L is length of combustion chamber)

3.3 Temperature

Contour of temperature with different size of combustion chambers are shown in Figure 4. In the figure shows that the increase of diameter and length, the high temperature area is increased as well because of more mixing area. Lower temperature area can be seen at center combustor axis and walls and extends to the walls of outlet pipes at D = 250 and 391 mm. It shows that the model is not effective for fuel-air mixing to complete combustion but at D=250 mm with maximum length, the contour shows good mixing more than other models that are mentioned. At D=600 in the other hand, is observed that there is no low temperature area at center combustor axis which means that the maximum diameter has a good air-fuel mixing more than small combustor diameter except the maximum combustor size because low tangential velocity, air-fuel mixing is not effective. The good mixing is observed at the end of combustor for maximum size because they are very different size between combustor diameter and outlet pipe diameter.

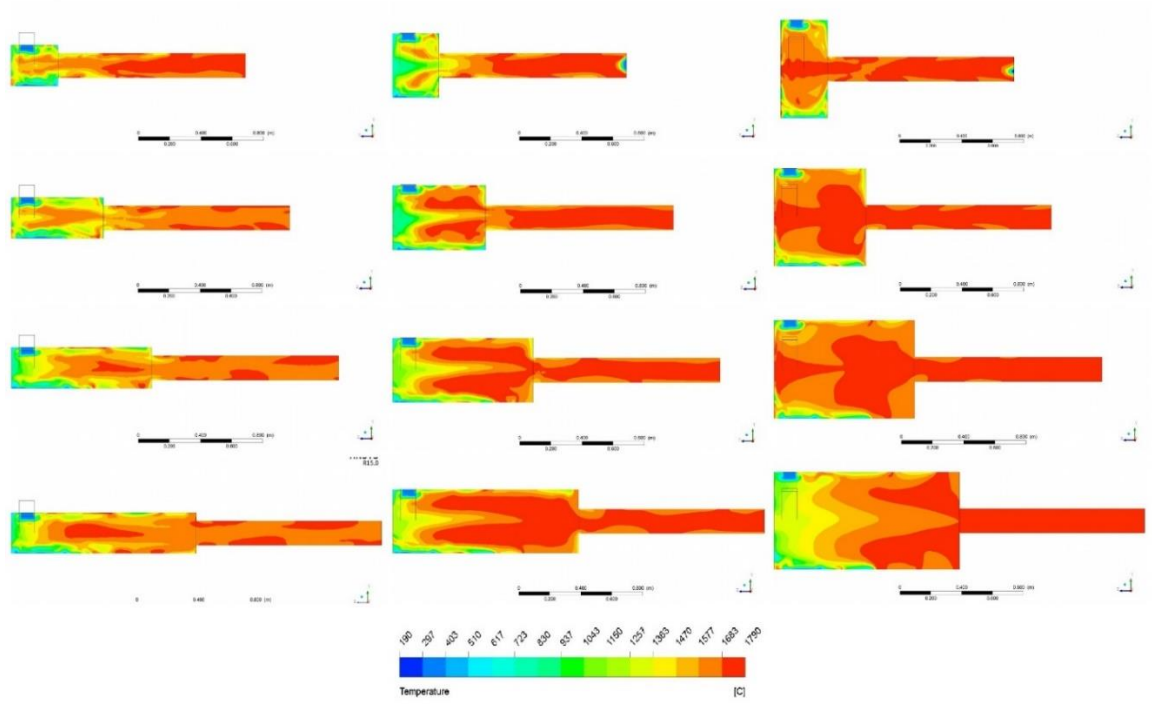

Figure 4 Temperature contour of models (M1-M12) follow Table 2

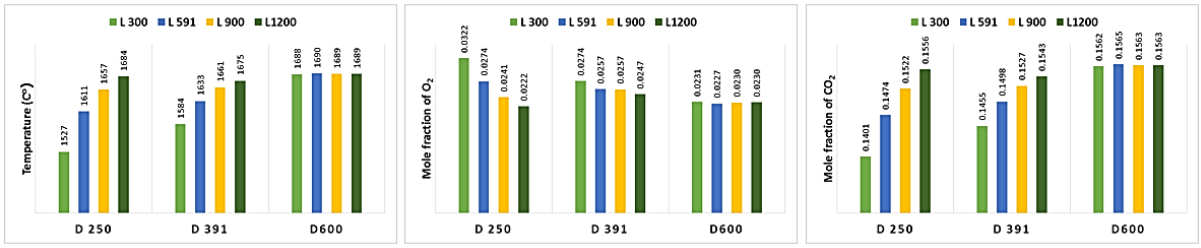

(a) (b) (c)

Figure 5 Result from numerical simulation (a) Temperature, (b) The mole fraction of O_2, (c) The mole fraction of CO_2 at 200 mm away from outlet of combustion chamber

3.4 Exhaust gas analysis

3.4.1 Temperature of exhaust gas

It should be noted that high temperature of exhaust gas is desired to maximize thermal energy. According to Figure 5 (a), the exhaust gas temperature increases when diameter and length of combustor are increased because resident time for chemical reaction is increased. But at D=391 and L= 1200 mm (M8) has resulted lower exhaust temperature comparing with other models at the same length, it results from pour mixing at the wall of combustor (Figure 3). Beside, all models at maximum diameter generate high exhaust gas temperature.

3.4.2 CO_2 and O_2 concentration

Figure 5 (b) and (c) show percentage of O_2 and CO_2 in exhaust gas at outlet respectively. The high percentage of CO_2 and low percentage of O_2 suggest that the combustion process have low burning efficiency. As it can be seen in the Figure 5 (c) CO_2 is directly proportional to the exhaust gas temperature (see Figure 5 (a)); in other word, the decrease of O_2, CO_2 is increased. It shows that high exhaust gas temperature is resulted from high burning efficiency due to high exhaust gas temperature resulting in high CO_2 and low O_2.

3.5 Comparison of exhaust gas temperature and volume of combustor

The effect of changing D and L of combustor causes the volume to change. Since the volume increases, increasing resident time in combustor (air-fuel mixing time is increased) causes high exhaust gas temperature. In the Figure 6 is obviously observed when the size of D is increased at the minimum L, the temperature at outlet is significantly increased due to the increasing of volume of combustor and the stronger flowing of cyclone. Similarly, when L is increased at the minimum D, the exhaust gas temperature is significantly increased because the fuel-air is mixed rapidly. Then the M4 model which has the smallest D and the longest L is the best one for minimizing the combustor volume and maximizing the exhaust gas temperature.

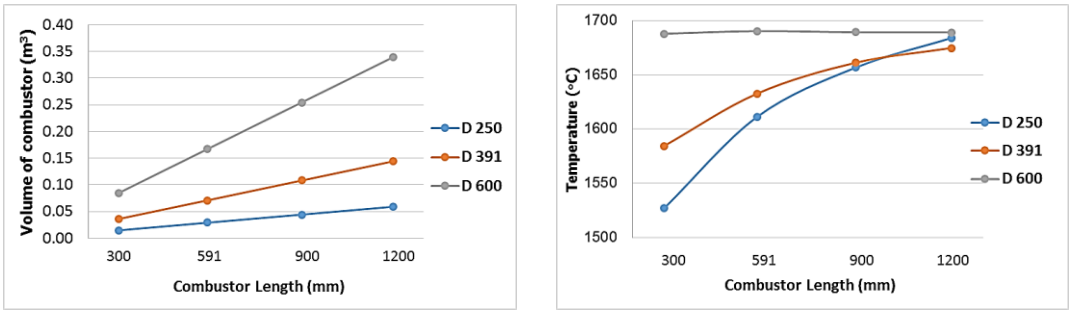

(a) (b)

Figure 6 (a) Combustor volume of each model. (b) The exhaust gas temperature at outlet

4. Conclusions

This study numerically investigated the effects of chamber dimensions to burn raw producer gas from gasifier. According to the result, it can be summarized in 2 cases as follows: the first is the increasing of burning efficiency; the combustor must have small volume but provides high outlet temperature. In this case, the model M4 is the most suitable. (D is small and L is long). The second case is inducing the strong vortex flow. The cyclonic flow in cyclone combustor can reduce the quantity of dust by centrifugal force; therefore, the combustor that has large D and short causes strong cyclonic flow.

5. Acknowledgements

The authors gratefully acknowledge the support of Mechanical Component Design Unit, Mechanical Engineering Department, Khon Kaen University for Ansys software for simulation.

6. References

[1] Prabhansu, Karmakar MK, Chandra P, Chatterjee PK. A review on the fuel gas cleaning technologies in gasification process. Journal of Environmental Chemical Engineering 2015;3(2):689-702.

[2] Guo X, Xiao B, Liu S, Hu Z, Luo S, He M. An experimental study on air gasification of biomass micron fuel (BMF) in a cyclone gasifier. *International* Journal of Hydrogen Energy 2009;34(3):1265-1269.

[3] Luo S, Xiao B, Hu Z, Liu S, He M. Experimental study on combustion of biomass micron fuel (BMF) in cyclone furnace. Energy Conversion and Management 2010;51(11):2098-2102.

[4] Al-attab KA, Zainal ZA. Design and performance of a pressurized cyclone combustor (PCC) for high and low heating value gas combustion. Applied Energy 2011;88(4):1084-1095.

[5] Madhiyanon T, Piriyarungroj N, Soponronnarit S. Cold flow behavior study in novel cyclonic fluidized bed combustor (ψ-FBC). Energy Conversion and Management 2008;49(5):1202-1210.

[6] Syred N, Beér, JM. Combustion in swirling flows: A review. Combustion and Flame 1974;23(2):143-201.

[7] Syred C, Fick W, Griffiths AJ, Syred N. Cyclone gasifier and cyclone combustor for the use of biomass derived gas in the operation of a small gas turbine in cogeneration plants. Fuel 2004;83(17-18):2381-2392.

[8] Dattarajan S, Kaluri R, Sridhar G. Development of a Combustor to burn raw producer gas. Fuel Processing Technology 2014;126:76-87.

[9] Chouaieb S, Kriaa W, Mhiri H, Bournot P. Presumed PDF modeling of microjet assisted CH4–H2/air turbulent flames. Energy Conversion and Management 2016;120:412-421.

[10] Obieglo A, Gass J, Poulikakos D. Comparative study of modeling a hydrogen nonpremixed turbulent flame. Combustion and Flame 2000;122(1-2):176-194.

[11] Khaleghi M, Hosseini SE, Abdul Wahid M. Investigations of asymmetric non-premixed meso-scale vortex combustion. Applied Thermal Engineering 2015;81:140-153.

[12] Warzecha P, Boguslawski A.. LES and RANS modeling of pulverized coal combustion in swirl burner for air and oxy-combustion technologies. Energy 2014;66:732-743.

[13] Choi B, Han Y, Kim M, Hwang C, Oh CB. Experimental and numerical studies of mixing and flame stability in a micro-cyclone combustor. Chemical Engineering Science 2009;64(24):5276-5286.

[14] Poinsot T, Veynante D. Theoretical and Numerical Combustion. 2nd ed. Philadelphia: R.T. Edwards Inc.; 2005.

[15] Ansys. Ansys fluent theory guide, version 14.5. Canonsburg, PA, USA: Ansys Inc; 2013.